THE ASTROPHYSICAL JOURNAL, 380:161–166, 1991 October 10

THE 10 YEAR RADIO LIGHT CURVES FOR SN 1979C

KURT W. WEILER AND SCHUYLER D. VAN DYK[1]
Center for Advanced Space Sensing, Naval Research Laboratory, Code 4215, Washington, DC 20375-5000
NINO PANAGIA[2,3]
Space Telescope Science Institute, 2700 San Martin Drive, Baltimore, MD 21218
RICHARD A. SRAMEK
National Radio Astronomy Observatory, Socorro, NM 87801
AND
JENNIFER L. DISCENNA[4]
Center for Advanced Space Sensing, Naval Research Laboratory, Code 4215, Washington, DC 20375-5000
Received 1991 April 9; accepted 1991 April 23

ABSTRACT

We present new observations of the radio supernova SN 1979C made with the VLA at $\lambda\lambda 20$, 6, and 2 cm from 1985 March through 1990 December, augmenting our previous observations which began only 8 days after optical maximum in 1979 April and extended through 1984 November. We find that the "mini-shell" model of Chevalier still provides the best representation of these more complete light curves at all three wavelengths. Shorter period fluctuations in the observations are real and are probably due to emission efficiency variations caused by structure in the presupernova stellar wind density. We also find evidence for more than 1 $M_\odot$ lost from the progenitor star in the presupernova stellar wind. This suggests that the star's mass was originally $M_{\rm ZAMS} \gtrsim 13\ M_\odot$. These observations represent the longest and most complete data set available for the emission from any supernova in any wavelength band.

Subject headings: nebulae: supernovae remnants — stars: individual (SN 1979C) — stars: radio radiation — stars: supernovae

1. INTRODUCTION

The study of supernovae (SNs, hereafter) which are significant sources of radio emission, known as "radio SNs" (RSNs), provides important information on the properties of the progenitor stellar systems and their immediate circumstellar environments, as well as on the connection between SNs, RSNs, and supernova remnants (SNRs; Weiler & Sramek 1988).

We discuss in this paper the specific case of SN 1979C [$\alpha(1950.0) = 12^h20^m26^s.71 \pm 0^s.01$; $\delta(1950.0) = +16°04'29''.5 \pm 0''.2$] in NGC 4321 (M 100). It was discovered near maximum light on 1979 April 19 by Johnson (1979), with an estimated date of maximum light of April 19 and an estimated date of explosion of 1979 April 4 (Weiler et al. 1986). We have monitored this supernova with the Very Large Array (VLA)[5] since 1979 April 27 at wavelengths $\lambda\lambda 20$, 6, and 2 cm. The results of our observations from that time through 1984 November are contained in Weiler et al. (1986). We present here our new monitoring results from 1985 March through 1990 December. These more complete light curves illustrate the evolution of radio emission from the Type II supernova SN 1979C over more than a decade.

Weiler et al. (1986) discuss the common properties that most RSNs apparently share. These include: (1) nonthermal emission with high brightness temperature; (2) light curve "turn-on" at shorter wavelengths first and longer wavelengths later; (3) an initial rapid increase of flux density with time at each wavelength, with a power-law decline after maximum is reached; and (4) a sharp initial decrease in spectral index between two wavelengths, as the longer wavelength emission goes from being optically thick to thin, with the spectral index value, α, asymptotically approaching an optically thin, nonthermal, constant negative value.

Two models have been proposed to explain the existing RSNs data: the "mini-shell" model and the "mini-plerion" model (Weiler et al. 1986). The "mini-shell" model (e.g., Chevalier 1981a, b; 1984a, b) involves the external generation of relativistic electrons and enhanced magnetic field necessary for synchrotron radio emission by the shock wave from the supernova explosion interacting with a relatively high-density surrounding envelope of matter. This envelope arises from mass loss in a stellar wind from the presupernova star before the explosion.

The "mini-plerion" model (e.g., Pacini & Salvati 1973, 1981; Shklovskii 1981; Marscher & Brown 1978; Bandiera, Pacini, & Salvati 1983, 1984) involves a central generation of relativistic electrons and enhanced magnetic field necessary for synchrotron radio emission by the remnant of the supernova progenitor star, which has become something like a rapidly rotating neutron star or pulsar. Such a mini-plerion might resemble a very young Crab Nebula.

Weiler et al. (1986) showed that, from the results through 1984, for SN 1979C the degenerate condition applied where both the mini-shell model and the mini-plerion model could

[1] Naval Research Lab/National Research Council Cooperative Research Associate.
[2] Affiliated with the Astrophysics Division, Space Science Department of ESA.
[3] Also University of Catania, Italy.
[4] Current address: Department of Physics & Astronomy, Michigan State University, East Lansing, MI 48824-1116.
[5] The VLA is operated by the National Radio Astronomy Observatory of Associated Universities, Inc., under a cooperative agreement with the National Science Foundation.

TABLE 1

CALIBRATION SOURCES

Source Name (1)	Calibrator Type (2)	$\alpha_{1950.0}$ (3)	$\delta_{1950.0}$ (4)	S_{20} (Jy) (5)	S_6 (Jy) (6)	S_2 (Jy) (7)
3C 286	Primary	Not used	Not used	14.45	7.42	3.45
1252+119[a]	Secondary	$12^h52^m07^s.724$	$+11°57'20''.82$	...	...	...

[a] See Table 2 for flux densities.

equally well fit the radio observations. Preference was given to the mini-shell model, based on the argument that the large amount of mass in the vicinity of a supernova explosion, even if only a small fraction of it were ionized, would totally prevent detection of radio emission from a centrally driven source. With the additional data from 1985 to 1990 presented here, we find that the 10 yr radio light curves for SN 1979C provide evidence that the mini-shell is appropriate and that the mini-plerion is to be excluded as a viable explanation for the radio emission in this case.

2. OBSERVATIONS

The new observations of SN 1979C were made with the VLA at $\lambda 20$ cm (1.490 GHz), $\lambda 6$ cm (4.860 GHz), and $\lambda 2$ cm (14.940 GHz) from 1985 March through 1990 December at a quarterly rate. Since monitoring of an evolving radio source requires measurement at frequent intervals, we were not able to request the VLA configuration and consequently have measurements at all array sizes. Along with each observation of the source, a short observation of a "secondary," possibly variable, calibrator, 1252+119, was made at each frequency. To establish an absolute flux density scale, each observing session also included an observation of the "primary," presumed constant, calibrator 3C 286.

2.1. *Calibration*

The VLA is described in a number of publications (e.g., Thompson et al. 1980; Hjellming & Bignell 1982; Napier, Thompson, & Ekers 1983); the general procedures for RSNs observations, with analysis of the possible sources of error, are discussed in Weiler et al. (1986). The "primary" calibrator employed here, 3C 286, was assumed to be constant in flux density with time and to have the flux densities at $\lambda\lambda 20$, 6 and 2 cm given in Table 1.

The "secondary" calibrator, 1252+119, was used as the phase (position) and amplitude (flux density) reference for the observations of SN 1979C. Its assumed position (epoch 1950.0) is given in Table 1, and its flux density values, measured against 3C 286, at $\lambda 20$ cm (S_{20}), $\lambda 6$ cm (S_6), and $\lambda 2$ cm (S_2) are presented for each observing date in Table 2. On two separate occasions (1985 March 18 and 1986 June 16) independent calibrations with 3C 286 were not available, and other means, described in footnotes to Table 2, were employed for determining calibration values.

2.2. *Data Reduction*

After the data were initially calibrated using standard software packages on the DEC-10 and Convex computers at the VLA, the data were "exported" to the NRL for analysis with AIPS on the local VAX 11/785 and Alliant VFX/40 computers. Most data sets were individually hand-edited, mapped, CLEANed, inspected, corrected with SELFCAL techniques using the compact emission of SN 1979C itself as a reference, then remapped, reCLEANed, and measured independently in both IF channels for each observing band. The values from the two IF channels were then averaged to obtain a final measurement of the flux density in each band at each epoch. Observations after 1989 April were not corrected using AIPS SELFCAL techniques and were mapped by combining both IF channels into a single map.

2.3. *Errors*

One estimate for the flux density measurement error is the rms "map" error which measures the contribution of small, unresolved fluctuations in the background emission and random map fluctuations due to receiver noise. This can only be considered a lower limit to the total error. Comparison of the two IF channel flux density solutions is clearly too small of a sample to provide meaningful statistics; also, the two IF channels do not provide truly independent solutions for a number of types of instrumental errors. Therefore, errors for the measurements in this paper include a basic 5% error to account for the normal inaccuracy of VLA flux density mea-

TABLE 2

MEASURED OR ASSUMED FLUX DENSITY VALUES FOR THE SECONDARY CALIBRATOR 1252+119

Observation Date (1)	S_{20} (Jy) (2)	S_6 (Jy) (3)	S_2 (Jy) (4)
1985 Mar 18[c]	0.950	0.642	...
1985 Jun 28[a]	0.950	0.643	...
1985 Aug 22[a]	0.936	0.635	...
1985 Dec 14[a]	0.992	0.652	...
1986 Mar 28[a]	0.900	0.634	...
1986 Jun 16[b]	0.920	0.632	...
1986 Sep 25[a]	0.938	0.630	...
1986 Dec 15[a]	0.954	0.641	...
1987 Mar 05[a]	...	0.643	0.428
1987 Jun 24[a]	0.842	0.606	...
1987 Sep 18[a]	0.865	0.605	...
1987 Dec 20[a]	0.870	0.592	...
1988 Mar 31[a]	0.897	0.618	...
1988 Sep 16[a]	0.887	0.630	0.372
1988 Dec 29[a]	0.898	0.594	...
1989 Apr 06[a]	0.893	0.566	...
1989 Jul 17[a]	0.802	0.526	...
1989 Dec 21[a]	...	0.549	...
1990 Feb 12[a]	...	0.590	...
1990 May 29[a]	0.800	0.560	...
1990 Dec 07[a]	0.801	0.593	...

[a] Calibrated independently using 3C 286.

[b] Not independently calibrated. Calibration values taken as an average of the results on 1986 Mar 28 and 1986 Sep 25.

[c] Not independently calibrated. Calibration values adopted from 1985 Jun 28.

TABLE 3

NEW FLUX DENSITY AND SPECTRAL INDEX MEASUREMENTS FOR SN 1979C[a]

Observation Date (1)	Time since Optical Maximum[b] (days) (2)	VLA Configuration (3)	Flux Density						Spectral Index ($S \propto \nu^{+\alpha}$)			
			S_{20} (mJy) (4)	σ_{20} (mJy) (5)	S_6 (mJy) (6)	σ_6 (mJy) (7)	S_2 (mJy) (8)	σ_2 (mJy) (9)	α_6^{20} (10)	$\sigma_{\alpha_6^{20}}$ (11)	α_2^6 (12)	$\sigma_{\alpha_2^6}$ (13)
1979 Apr 19	≡ 0	...	...	...	...	...	...	...	...	...	...	...
1980 Aug 5	473	...	...	...	...	...	...	...	...	...	− 0.83	0.30
1980 Dec 4	594	...	...	...	...	...	...	...	...	...	− 0.75	0.30
1981 Sep 12	876	...	...	...	...	...	...	...	...	...	− 0.82	0.17
1984 Feb 12	1750	...	...	...	...	...	...	...	...	...	− 0.74	0.14
1985 Mar 18	2160	A/B	8.40	0.53	3.61	0.21	...	...	− 0.71	0.07	...	...
1985 Jun 28	2262	B/C	7.34	0.71	3.49	0.22	...	...	− 0.63	0.10	...	...
1985 Aug 22	2317	C	5.64	0.67	3.60	0.23	...	...	− 0.38	0.11	...	...
1985 Dec 14	2431	D	8.58	0.96	3.00	0.19	...	...	− 0.89	0.11	...	...
1986 Mar 28	2535	A	7.18	0.39	3.67	0.20	...	...	− 0.57	0.07	...	...
1986 Jun 16	2615	A/B	6.30	0.48	3.95	0.24	...	...	− 0.39	0.08	...	...
1986 Sep 25	2716	B/C	7.58	0.63	3.40	0.19	...	...	− 0.68	0.08	...	...
1986 Dec 15	2797	C	7.39	0.77	3.19	0.19	...	...	− 0.71	0.10	...	...
1987 Mar 05	2877	D	...	...	2.77	0.17	1.11	0.16	...	...	− 0.81	0.14
1987 Jun 24	2988	A	6.93	0.41	3.58	0.22	...	...	− 0.56	0.07	...	...
1987 Sep 18	3074	A	6.12	0.35	2.50	0.16	...	...	− 0.76	0.07	...	...
1987 Dec 20	3167	B	5.34	0.37	2.90	0.17	...	...	− 0.52	0.08	...	...
1988 Mar 31	3269	C	5.55	0.70	2.70	0.16	...	...	− 0.61	0.12	...	...
1988 Sep 16	3438	D	...	...	2.19	0.16	0.66	0.35	...	...	− 1.07	0.48
1988 Dec 29	3542	A	5.26	0.31	2.13	0.14	...	...	− 0.77	0.08	...	...
1989 Apr 06	3640	B	4.73	0.44	2.61	0.15	...	...	− 0.50	0.09	...	...
1989 Jul 17	3742	C	3.96	0.36	1.83	0.12	...	...	− 0.65	0.10	...	...
1989 Dec 21	3899	D	...	...	2.24	0.15	...	...	...	...	...	...
1990 Feb 12	3952	D/A	...	...	1.90	0.18	...	...	...	...	...	...
1990 May 29	4058	A	5.80	0.31	2.30	0.14	...	...	− 0.78	0.07	...	...
1990 Dec 07	4250	C	4.71	0.46	2.39	0.13	...	...	− 0.57	0.10	...	...

[a] For previous measurements, cf. Weiler et al. 1986.

[b] The date of the explosion is taken to be 1979 Apr 4, 15 days before optical maximum (cf. Weiler et al. 1986).

surements and any absolute scale error for the primary calibrator, 3C 286. The final errors, σ_f, listed in Table 3, are taken as

$$\sigma_f^2 \equiv (0.05S_0)^2 + \sigma_0^2 , \quad (1)$$

where S_0 is the observed flux density for SN 1979C and σ_0 is the observed rms map error measured outside of any obvious regions of emission.

One final source of error which had to be taken into account might be called the "configuration" error. At long wavelengths and short baselines (i.e., low resolving power), the contribution of the flux density per beam area from the disk emission of NGC 4321, particularly from the spiral arm just to the north of SN 1979C, had to be considered. The measurement procedure of subtracting a background emission estimate from the measured flux density value for SN 1979C appears to be adequate, since, as in Weiler et al. (1986), we do not find any systematic trend between measured flux density and VLA configuration.

3. RESULTS

Since the previous publication of SN 1979C data, in Weiler et al. (1986), we have added 14 new measurements at $\lambda 20$ cm, 16 new measurements at $\lambda 6$ cm, and two new measurements at $\lambda 2$ cm. We present these in Table 3. Column (1) is the date of observation; column (2) is the time, in days, since optical maximum (the date of explosion is taken by Weiler et al. to have been ~ 15 days before optical maximum, or $\sim$ 1979 April 4); column (3) gives the VLA configuration in which the supernova was observed; columns (4), (6), and (8) give the measured flux densities at $\lambda 20$ cm (S_{20}), $\lambda 6$ cm (S_6), and $\lambda 2$ cm (S_2), respectively; and columns (5), (7), and (9) give the error estimates for these measurements.

Table 3 also contains determinations of spectral index, α, from our data ($S \propto \nu^{+\alpha}$), with column (10) listing the spectral index, α_6^{20}, between $\lambda\lambda 20$ and 6 cm, and column (11), its error, $\sigma_{\alpha_6^{20}}$; and column (12) listing the spectral index, α_2^6, between $\lambda\lambda 6$ and 2 cm, and column (13), its error, $\sigma_{\alpha_2^6}$. Several older determinations of the spectral index available to Weiler et al. (1986), in their Table 4, but not explicitly calculated by them, are listed at the top of Table 3.

In Figure 1 we plot the time evolution of the flux density of SN 1979C in all three radio bands, including both the new results and the results for earlier epochs from Weiler et al. (1986). The solid lines are the "best fit" model light curves discussed below. In Figure 2 we show the change in spectral index between $\lambda\lambda 20$ and 6 cm with time over the decade since explosion. One can see from Figure 2 that the spectral index change is very similar to that found by Weiler et al. (1986), with α_6^{20} asymptotically approaching a value of ~ -0.75. The solid curve shown in Figure 2 is not an independent fit, but is calculated from the model light curves shown in Figure 1. In Figure 3 we show the time evolution of the spectral index, α_2^6. As can be seen in Table 3, the gas has been optically thin to emission at these two wavelengths, with the spectral index remaining essentially $\alpha_2^6 \sim -0.8$, throughout the decade of observations.

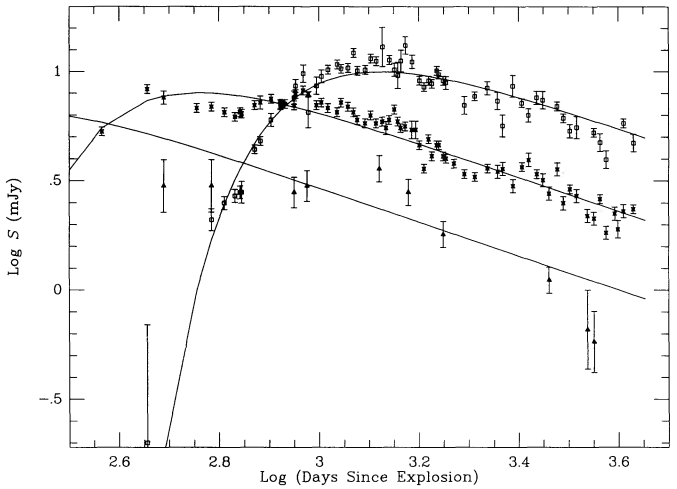

FIG. 1.—Radio "light curves" for SN 1979C in NGC 4321 (M 100). The three wavelengths, $\lambda 20$ cm (*open squares*), $\lambda 6$ cm (*4 sided stars*), and $\lambda 2$ cm (*filled triangles*), are shown together. Data represent more than 10 yr of observations for this object, including new observations presented in this paper and previous observations from Weiler et al. (1986). Age of the supernova is measured in days from the estimated date of explosion on 1979 April 4 (15 days before optical maximum). Solid lines represent the best-fit light curves of the form $S(\mathrm{mJy}) = K_1[\nu/(5\ \mathrm{GHz})]^{\alpha}[(t - t_0)/(1\ \mathrm{day})]^{\beta}e^{-\tau}$, where $\tau = K_2[\nu/(5\ \mathrm{GHz})]^{-2.1}[(t - t_0)/(1\ \mathrm{day})]^{\delta}$, and $\delta \equiv \alpha - \beta - 3$.

4. DISCUSSION

4.1. *Light Curves*

Following Weiler et al. (1986) we assume:

1.—That the radio emission is due to the nonthermal synchrotron process with optically thin spectral index, α;

2.—That the absorption or optical depth, τ, is purely of a thermal, free-free nature in an ionized medium (frequency dependence $\nu^{-2.1}$) external to the emitting region with a radial density dependence $\rho \propto r^{-2}$ from a red supergiant wind of constant speed; and

3.—That the observed flux density, S, and the optical depth, τ, can be well described as functions of supernova age, $t - t_0$,

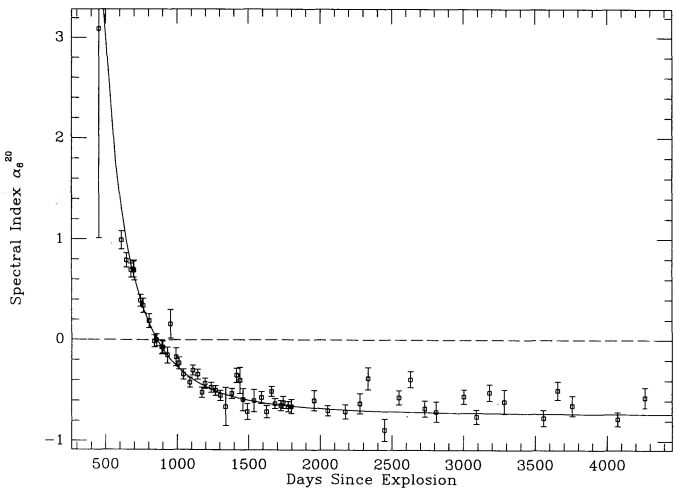

FIG. 2.—Spectral index α ($S \propto \nu^{+\alpha}$) evolution for SN 1979C between 20 and 6 cm, plotted as a function of time, in days, since the estimated explosion date of 1979 April 4 (15 days before optical maximum). The solid line is calculated from the best-fit theoretical "light curves" shown in Fig. 1. The dashed line shows $\alpha = 0$.

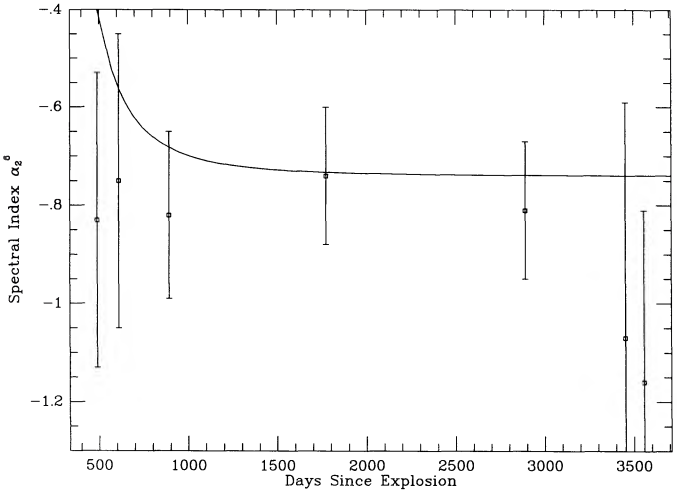

FIG. 3.—Spectral index α ($S \propto \nu^{+\alpha}$) evolution for SN 1979C between 6 and 2 cm, plotted as a function of time, in days, since the estimated explosion date of 1979 April 4 (15 days before optical maximum). The solid line is calculated from the best-fit theoretical "light curves" shown in Fig. 1.

to the powers β and δ, respectively, after an explosion epoch t_0. This formulation can be written as

$$S(\mathrm{mJy}) = K_1\left(\frac{\nu}{5\ \mathrm{GHz}}\right)^{\alpha}\left(\frac{t - t_0}{1\ \mathrm{day}}\right)^{\beta}e^{-\tau}, \quad (2)$$

where

$$\tau = K_2\left(\frac{\nu}{5\ \mathrm{GHz}}\right)^{-2.1}\left(\frac{t - t_0}{1\ \mathrm{day}}\right)^{\delta}. \quad (3)$$

The factors K_1 and K_2 above are scaling parameters for the units of choice (mJy, GHz, and days) and formally correspond to the flux density and optical depth, respectively, at 5 GHz, one day after explosion.

Mixed, internal absorbing and emitting processes could not cause the initial radio light curve to rise as quickly as observed (cf. Marsher & Brown 1978), and, if the location of the absorbing material is external, only a thermal process is possible. The two nonthermal processes for absorption, the Razin-Tsytovich effect and synchrotron self-absorption, require densities that are impossibly high for regions surrounding a supernova (cf. Marscher & Brown 1978; Chevalier 1982a, b; Bandiera et al. 1984). The single known RSN exception to this purely external, thermal absorption behavior is SN 1986J, which appears to require mixed, internal, nonthermal emitting/thermal absorbing gas. SN 1986J is described in detail elsewhere (Weiler, Panagia, & Sramek 1990).

The full available data set at $\lambda\lambda 20$, 6, and 2 cm, including the values from Weiler et al. (1986), was then used to solve for the four free parameters, K_1, K_2, α, and β, in equations 2 and 3. The date of explosion, t_0, is not well constrained by the data and, following Weiler et al. (1986), was defined to be 1979 April 4. Because of the success of the Chevalier model (Chevalier 1981a, b; 1984a, b) for RSNs emission (see also Weiler et al. 1986; Weiler et al. 1990), δ was not solved for, but was taken to be (Chevalier 1984b)

$$\delta \equiv \alpha - \beta - 3. \quad (4)$$

The "best" fit was obtained by using a minimum reduced χ^2 procedure to identify the best value and range of values for each of the parameters. These values, which are listed in Table

TABLE 4

FITTING PARAMETERS FOR SN 1979C[a,b]

Parameter (1)	Value (2)	Deviation Range[c] (3)
K_1	1446	1080–1770
α	−0.74	−(0.66–0.79)
β	−0.78	−(0.76–0.81)
K_2	3.64×10^7	$(2.40–6.83) \times 10^7$
$\delta(\equiv \alpha - \beta - 3)$	−2.96	−(2.85–3.03)
t_0[d]	≡ 1979 Apr 4	

[a] The radio light curves are assumed to fit a curve of the form S (mJy) $= K_1[\nu/5\ \text{GHz}]^{\alpha}[t - t_0]^{\beta}e^{-\tau}$, where $\tau = K_2[\nu/5\ \text{GHz}]^{-2.1}[t - t_0]^{\delta}$. From Chevalier 1984b, $\delta \equiv \alpha - \beta - 3$ is assumed.

[b] With an error of 10.5% for the measured flux densities to account for the fact that no simple model can completely describe such a complicated phenomenon, these parameters yield a $\chi^2_{\text{red}} \simeq 1.2$.

[c] The deviation range is the range in which there is a ~67% probability that the true value lies. This is equivalent to a 1 σ range for a one parameter solution.

[d] The date of the explosion is taken to be 1979 Apr 4, following Weiler et al. 1986. Due to relatively few points being available at early epochs, t_0 is poorly determined by the model fit.

4, were computed assuming a minimum measurement error of 10.5% to give a $\chi^2_{\text{red}} \sim 1$ per degree of freedom. This need to increase the data errors beyond the measurement level of ~5% in order to obtain a $\chi^2_{\text{red}} \sim 1$ implies, not unexpectedly, that the model of equations 2 and 3 is not sufficiently complex to describe the details of short-term fluctuations in the light curves (see § 4.3 below). The range of uncertainty listed for each parameter is the amount that a parameter must deviate from the best-fit value in order to increase χ^2_{red} from ~1 to ~5 (Abramowitz & Stegun 1965). This is appropriate for a four parameter fit and determines the 67% probability intervals within which the true values lie; that is, the error range analogous to the 1 σ uncertainty for a single parameter fit. The model curves calculated in equations 2 and 3 for the parameter values of Table 4 are shown as the solid lines in Figure 1.

Examination of Figures 1, 2, and 3 show that the model curves, even for such a simple model, describe the available data at all frequencies very well in gross terms. The parameters listed in Table 4, in fact, agree with those determined for the more limited data set available to Weiler et al. (1986) to within the fitting uncertainties (Weiler et al. give $K_1 = 930 \pm 120$, $\alpha = -0.72 \pm 0.05$, $\beta = -0.71 \pm 0.08$, and $K_2 = [5.1 \pm 0.3] \times 10^7$). The radio emission of SN 1979C is clearly evolving in a regular manner, albeit with small, short-term fluctuations about the general trend. There have been no extreme brightenings or fadings caused by large density fluctuations in the red supergiant wind or by approaching the wind's outer boundary. The wind boundary, at which Weiler et al. (1986) predicted that the radio emission should sharply cut off, has clearly not yet been reached.

4.2. *Models*

As discussed above, two models, the mini-shell and the mini-plerion, have been suggested to provide the mechanism for the acceleration of the relativistic particles generating the non-thermal emission from SN 1979C. In general terms, the flux density is a power-law function of both frequency and time, with the form

$$S \propto \nu^{\alpha} t^{\beta} . \tag{5}$$

For the case of the mini-shell model,

$$\beta = -(\gamma + 5 - 6m)/2 = -(3 - 3m - \alpha) , \tag{6}$$

and

$$\alpha = (1 - \gamma)/2 , \tag{7}$$

where α is the optically thin radio spectral index, m is the exponent in the time-dependent relation for the supernova shock front radius, $R \propto t^m$ (Chevalier 1982a, b; also, $\delta = -3m$), and γ is the exponent of the power law of the relativistic electron energy spectrum (e.g., Chevalier 1984b).

The mini-plerion model has the form of equation (5) with

$$\beta = (1 - \gamma/2)(3m - 1)/2 , \tag{8}$$

and

$$\alpha = -\gamma/2 , \tag{9}$$

for $\nu > \nu_b$, where m and γ are as defined above; and

$$\beta = \alpha + 3(1 - \alpha)(1 - m)/2 , \tag{10}$$

$$\alpha = (1 - \gamma)/2 , \tag{11}$$

for $\nu < \nu_b$, where m and γ are again as defined above. The term ν_b is a discontinuity, or critical "break," frequency, at which adiabatic losses and synchrotron losses become equal (cf. Pacini & Salvati 1973).

The mini-plerion case, for which $\nu > \nu_b$, can be ruled out, since, as was demonstrated in Weiler et al. (1986), the model predicts, for the "best fit" to the observations of SN 1979C, a constant or increasing flux density with time, which is clearly not observed. However, Weiler et al. (1986), were not able to distinguish from their model fit parameters in the four parameter case (Chevalier 1984b) between the mini-plerion model with $\nu < \nu_b$ and the mini-shell model. They had to rely on other arguments to show preference for the mini-shell model. Their best value for m ($\equiv -\delta/3 = -(\alpha - \beta - 3)/3$) of 1.00 for SN 1979C was the degenerate, undecelerated ejecta case, where the mini-shell and mini-plerion models give the same predictions. With our new data and model fits, however, this degeneracy is broken, with a best value of $m = 0.987\ (+0.023, -0.037)$. With $\alpha = -0.74$, $\beta = -0.78$ (see Table 4), and $m = 0.987$, examination of Table 10 in Weiler et al. (1986) shows that the mini-plerion model with $m < 1.00$ predicts $|\beta| < |\alpha|$, which is not observed (cf. Table 4). On the other hand, the mini-shell model with $m < 1.00$ predicts $|\beta| > |\alpha|$, which reference to Table 4 shows to be the case, confirming our previous faith in the mini-shell model for SN 1979C.

4.3. *Short-Period Light Curve Deviations*

Even though Figures 1 and 2 show a very regular long-term behavior for the radio emission from SN 1979C, some short-period deviations do occur, as was noted by Weiler et al. (1986). In Figure 4 we show the percentage difference, $([S_{\text{obs}} - S_{\text{model}}]/S_{\text{model}}) \times 100$, between the observed flux densities and the model flux densities at both λ6 and λ20 cm.

It is interesting to note that the deviations of the observed flux densities from the model curves are relatively well correlated between λ6 and λ20 cm and exhibit a quasi-periodic behavior. The deviations are mainly negative around 600, 2100, and 3600 days since explosion and are generally positive around 1200 and 2700 days since explosion. A power spectral analysis of the deviations, in fact, shows a significant sinusoidal component at both frequencies with a period of ~1540 days. On the other hand, examination of the spectral index in Figure

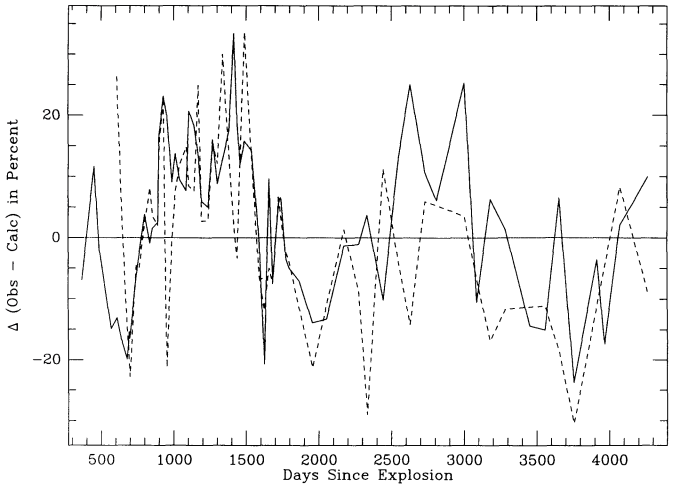

FIG. 4.—Deviations in percent, $([S_{obs} - S_{model}]/S_{model}) \times 100$, of the observed flux density values from the best-fit model values at both $\lambda 6$ cm (*solid line*) and $\lambda 20$ cm (*dashed line*).

2 reveals no such systematic modulation, implying that the flux density changes are due to a modulation of the emission efficiency, as suggested by Weiler et al. (1986), rather than due to a change in the optical depth of the external medium, as was seen by Weiler et al. (1990) in the case of SN 1986J. This quasi-periodic behavior for the emission from SN 1979C can, in fact, account for most of the "minimum measurement error of 10.5%," which we found necessary to introduce into the fitting procedure (see § 4.1) to give a $\chi^2_{red} \sim 1$ per degree of freedom for our simple model (eqs. 2 and 3). Because such a possible periodic variation in the radio emission efficiency has significant implications for modulation of the presupernova stellar mass-loss rate, we will reserve more detailed discussion and possible model interpretations for a separate paper.

4.4. *The Mass of the Progenitor*

An estimate of the mass-loss rate for the assumed presupernova red supergiant progenitor star can be made using the simplified formula of equation (16) in Weiler et al. (1986). Adopting a wind velocity, $w \sim 10$ km s^{-1}, an optical expansion velocity of the supernova ejecta, $v_i \simeq 9.2 \times 10^3$ km s^{-1} (cf. Weiler et al. 1986), and an electron temperature in the wind, $T \sim 3 \times 10^4$ K (Lundqvist & Fransson 1988), the mass loss is then $\dot{M} \simeq 1.2 \times 10^{-4}\ M_\odot$ yr^{-1}. Assuming that the wind velocity, w, during this mass loss was constant, the duration of this mass loss epoch, $\Delta t_{\dot{M}}$, is the ratio of the radius of the wind-blown circumstellar shell, R_{shell}, to the velocity w. A lower limit can now be placed on R_{shell} from the known time of interaction of the SN ejecta with the shell material. This minimum time of interaction is, of course, the duration of the radio emission from the RSN, $\Delta t_{radio} = 11.6$ yr. If the ejecta velocity is assumed to be constant, then $R_{shell} \gtrsim 3.4 \times 10^{17}$ cm and the duration of high mass loss is $\Delta t_{\dot{M}} \gtrsim 1.1 \times 10^4$ yr. With the estimate of the mass-loss rate above, we can place a lower limit on the amount of mass lost from the progenitor, assumed to occur during the red supergiant phase, of $\Delta M \gtrsim 1.3\ M_\odot$. From the stellar evolution models of Maeder & Meynet (1988) for stars with solar metallicity, this implies that the stellar progenitor for SN 1979C had a zero-age main-sequence mass of $M_{ZAMS} \gtrsim 13\ M_\odot$.

5. CONCLUSIONS

Analysis of the radio emission from the Type II radio supernova SN 1979C at $\lambda\lambda 20$, 6 and 2 cm leads to the following conclusions:

1.—The emission from SN 1979C is continuing its regular decline in flux density with time.

2.—The light curves, including the most recent data, are still consistent with the model for nonthermal emission with external, thermal absorption.

3.—The best-fit parameters differ only slightly, and within the statistical errors, from the values obtained by Weiler et al. (1986), indicating that the model is still accurate 10 yr after explosion.

4.—The earlier choice of the mini-shell model to describe the nonthermal emission for SN 1979C is now supported by the fitting parameter values.

5.—Shorter period fluctuations in the light curves are real and are probably due to emission efficiency variations, rather than optical depth effects.

6.—The red supergiant progenitor for SN 1979C maintained a very high mass-loss rate of greater than $10^{-4}\ M_\odot$ yr^{-1} for at least 10^4 yr before explosion.

7.—More than 1 $M_\odot$ can be accounted for as having been lost from the progenitor in the presupernova stellar wind.

8.—The zero-age main-sequence mass of the progenitor of SN 1979C was probably $\gtrsim 13\ M_\odot$.

In summary, with the longest and most complete data set available for emission from any supernova in any wavelength band we are able to strengthen our understanding of Type II RSNs and their interaction with their local environments.

REFERENCES

Abramowitz, M., & Stegun, I. A. 1965, Handbook of Mathematical Functions (New York: Dover), 980
Bandiera, R., Pacini, F., & Salvati, M. 1983, A&A, 126, 7
———. 1984, ApJ, 285, 134
Chevalier, R. A. 1981a, ApJ, 246, 267
———. 1981b, ApJ, 251, 259
———. 1982a, ApJ, 259, 302
———. 1982b, ApJ, 259, L85
———. 1984a, Ann. NY Acad. Sci., 422, 215
———. 1984b, ApJ, 285, L63
Hjellming, R. M., & Bignell, R. C. 1982, Science, 216, 1279
Johnson, G. E. 1979, IAU Circ. No. 3348
Lundqvist, P., & Fransson, C. 1988, A&A, 192, 221
Maeder, A., & Meynet, G. 1988, A&AS, 76, 411
Marscher, A. P., & Brown, R. L. 1978, ApJ, 220, 474
Napier, P. J., Thompson, A. R., & Ekers, R. D. 1983, Proc. IEEE, 71, 1295
Pacini, F., & Salvati, M. 1973, ApJ, 186, 249
———. 1981, ApJ, 254, L107
Shklovskii, I. S. 1981, Soviet Astr. Letters, 7 (4), 263
Thompson, A. R., Clark, B. G., Wade, C. M., & Napier, P. J. 1980, ApJS, 44, 151
Weiler, K. W., Panagia, N., & Sramek, R. A. 1990, ApJ, 364, 611
Weiler, K. W., & Sramek, R. A. 1988, ARA&A, 26, 295
Weiler, K. W., Sramek, R. A., Panagia, N., van der Hulst, J. M., & Salvati, M. 1986, ApJ, 301, 790